Eur. Phys. J. B **36**, 401–410 (2003)
DOI: 10.1140/epjb/e2003-00359-0

THE EUROPEAN PHYSICAL JOURNAL B

Interplay between phase ordering and roughening on growing films

B. Drossel[1,a] and M. Kardar[2]

[1] Institut für Festkörperphysik, TU Darmstadt, Hochschulstr. 6, 64289 Darmstadt, Germany
[2] Department of Physics, Massachusetts Institute of Technology, Cambridge, Massachusetts 02139

Received 23 July 2003
Published online 23 December 2003 –

Abstract. We study the interplay between surface roughening and phase separation during the growth of binary films. Renormalization group calculations are performed on a pair of equations coupling the interface height and order parameter fluctuations. We find a larger roughness exponent at the critical point of the order parameter compared to the disordered phase, and an increase in the upper critical dimension for the surface roughening transition from two to four. Numerical simulations performed on a solid-on-solid model with two types of deposited particles corroborate some of these findings. However, for a range of parameters not accessible to perturbative analysis, we find non-universal behavior with a continuously varying dynamic exponent.

PACS. 68.35.Rh Phase transitions and critical phenomena – 05.70.Jk Critical point phenomena – 05.70.Ln Nonequilibrium and irreversible thermodynamics – 64.60.Cn Order-disorder transformations; statistical mechanics of model systems

1 Introduction

Thin solid films are grown for a variety of technological applications, using molecular beam epitaxy (MBE) or vapor deposition. In order to create materials with specific electronic, optical, or mechanical properties, often more than one type of particle is deposited. When the particle mobility in the bulk is small, surface configurations become frozen in the bulk, leading to anisotropic structures that reflect the growth history, and are different from bulk equilibrium phases. If, for instance, a combination of particles are deposited that tend to phase separate at the surface, the grown films have lamellae or columns of the two phases that extend parallel to the growth direction [1,2]. This process of phase separation, as well as other ordering phenomena, can be affected by elastic forces, by the orientation of the growing crystal, by properties of the substrate, and by surface roughness. The range of possible scenarios is very rich and far from understood. There are a variety of analytical and computer models which try to shed light on some of these phenomena, but a systematic study and understanding of the possible phase transitions does not yet exist.

In this paper, we focus on the interplay between phase separation and surface roughening, neglecting the possible influence of elastic forces, substrate properties, and orientation dependencies due to the crystal structure. There exist several theoretical studies of phase separation during growth that neglect also the effect of surface roughness. In all these models it is assumed that the mobility of the atoms in the bulk is zero, such that all of the dynamics occurs at the surface. A model in which the probability that an incoming atom sticks to a given surface site depends on the state of the neighboring sites in the layer below [3], leads to a phase separation transition in the universality class of ordinary Ising models, if the model is symmetric with respect to the two phases. The same conclusion applies a model in which the top layer is fully thermally equilibrated before the next layer is added [4]. A model for spinodal decomposition during growth was introduced in reference [5]. In this model, phase separation is due to surface diffusion, and is limited due to the current of incoming particles, leading to a characteristic scale for the thickness of lamellae or columns, as confirmed by Monte-Carlo simulations [6].

However, the layer by layer growth mode underlying these models is unstable, and growing surfaces generally are rough. Several studies exist that investigate growth models that contain both phase separation and surface roughness. Simulations of an Eden model with two types of particles suggest that the surface roughness increases due to the phase separation [7]. A solid-on-solid growth model where the adsorption probabilities for the two types of particles depend on the local neighborhood in the layer below leads also to an increased surface roughness [8]. The reason is that particles are more likely to be adsorbed within

[a] e-mail: barbara.drossel@physik.tu-darmstadt.de

domains than at domain boundaries. On length scales much larger than the domain size, a crossover to the scaling behavior of the Kardar-Parisi-Zhang (KPZ) equation [9] is found. Another computer model where particles are adsorbed randomly and subsequently diffuse along the surface leads to domains whose thickness is a non-monotonous function of the deposition rate and the temperature, and for a certain range of parameter values, the height profile has steep steps at domain boundaries [10]. A set of coupled Langvin equations for this model is suggested in reference [11] and studied using stability analysis and Fourier decomposition.

These studies are rather incomplete, and in particular lacking a discussion of the possible effects of the height profile on the phase separation dynamics. A first attempt to a systematic study of the possible phases and scaling behaviors of coupled phase separation and roughening during growth was presented in a recent letter by us [12]. A set of two coupled Langevin equations was suggested, and computer simulations in 1+1 dimensions were performed, revealing a rich phase diagram. It is the purpose of this paper to extend and deepen this short study by presenting a renormalization group (RG) analysis, and further simulation results. While the RG analysis gives information about the behavior of the system in dimensions close to 4+1 and higher, computer simulations are particularly efficient in low dimensions. The general results obtained by the two approaches are compatible with each other. In addition, the computer simulations in 1+1 dimension reveal interesting nonuniversal behavior for a range of parameters that cannot be studied using perturbative RG.

The outline of the paper is as follows: In Section 2, we introduce and discuss the coupled set of Langevin equations used in this paper. Scaling laws and critical exponents will also be defined. Section 3 presents results of the RG analysis of these equations. One of the main findings is that the lower critical dimension for the surface roughening transition is increased from 2 to 4 dimensions due to the coupling to the critical phase ordering dynamics. Section 4 presents results of computer simulations. Section 5 analyses the connection of our model with the advection of a passive scalar in a velocity field, and with directed polymers drifting through a random medium. Section 6 contains a summary and discussion of our results.

2 Equations of motion and scaling laws

We consider the growth of a binary alloy on a d-dimensional substrate. Let $\mathbf{x}$ be the coordinate perpendicular to the growth direction, and t the time. Since we assume that all dynamics occurs at the surface of the growing material, the equations of motion can be expressed in terms of $\mathbf{x}$ and t alone. In order to characterize surface roughness and phase ordering, we introduce the height variable $h(\mathbf{x},t)$, which is the surface profile at position $\mathbf{x}$ at time t, and an order parameter $m(\mathbf{x},t)$, which is the difference in the densities of the two particle types at the surface at position $\mathbf{x}$ and time t. The interplay between the fluctuations in m, and the height h is captured phenomenologically by the coupled Langevin equations,

$$\partial_t h = \nu\nabla^2 h + \frac{\lambda}{2}(\nabla h)^2 + \frac{\alpha}{2}m^2 + \zeta_h, \tag{1}$$

$$\partial_t m = K(\nabla^2 m - rm - um^3) + a\nabla h\cdot\nabla m + bm\nabla^2 h + \frac{c}{2}m(\nabla h)^2 + \zeta_m, \tag{2}$$

with

$$\langle\zeta_h(\mathbf{x},t)\zeta_h(\mathbf{x}',t')\rangle = 2D_h\delta^d(\mathbf{x}-\mathbf{x}')\delta(t-t'),$$
$$\langle\zeta_m(\mathbf{x},t)\zeta_m(\mathbf{x}',t')\rangle = 2D_m\delta^d(\mathbf{x}-\mathbf{x}')\delta(t-t').$$

Since we are interested in the critical behavior of the model, we have assumed that it has the symmetry $m\to -m$, and included all potentially relevant terms compatible with this symmetry. In experiments or computer simulations, this symmetry can be achieved by tuning the ratio between the two types of adsorbed particles to the appropriate value. In the absence of such an order parameter symmetry, the system may undergo a first-order phase transition which is not considered here. Equation (1) is the Kardar-Parisi-Zhang (KPZ) equation [9] for surface growth, plus the leading coupling to the order parameter. Equation (2) is the time dependent Landau–Ginzburg equation for a (non-conserved) Ising model, with three different couplings to the height fluctuations. The Gaussian, delta-correlated noise terms, ζ_h and ζ_m, mimic the effects of faster degrees of freedom.

These equations apply to growth by vapor deposition, with particles sticking at surface sites with a probability that depends on the local environment in the growing film. The coupling terms in the Langevin equations (1) and (2) have obvious meaning in this context: The term proportional to α implies that particles are more likely to be absorbed within domains where they feel a stronger attractive force (if $\alpha > 0$). A negative α can also be meaningful: if the adsorption rate within domains is limited by the availability of particles of the correct type, this can slow down growth. However, if this is due to the vapor phase not being well stirred, additional equations for the particle concentrations in the vapor phase will be needed. Such equations are not included in this paper. The contribution from a (with $a > 0$) implies that domain walls tend to be driven downhill; e.g. if the identity of a newly adsorbed particle is more likely to be affected by its uphill neighbors than by the downhill ones. A positive b indicates that new domains are more likely to be formed in hilltops where there are less neighbors that could influence the type of particle to be adsorbed. The term proportional to c is similar in character to the KPZ nonlinearity λ, and means that susceptibility to phase separation depends on the slope.

Models for MBE typically assume that particle deposition at the surface is random, and that no desorption of particles takes place. In this case, the height profile and the order parameter dynamics are shaped by diffusion of particles along the surface. This physical situation leads

to a different set of Langevin equations,

$$\partial_t h = \nu\nabla^2 h + \frac{\beta}{2}\nabla^2 m^2 + \zeta_h, \tag{3}$$

$$\partial_t m = K\nabla^2 m - vm + \zeta_m, \tag{4}$$

where we have again imposed the symmetry $m \to -m$. The noise terms ζ_m and ζ_h have the same nonconserved correlations as for the vapor-deposition model above, due to the incoming particle current. Because of the conservation of volume during surface diffusion, the deterministic terms on the right-hand side of equation (3) must be the divergence of a current, disallowing the terms proportional to λ and α in equation (1). A negative value of β means that particles are more likely to be adsorbed within domains if they are not needed to the same extent in the neighborhood. The equation for the order parameter has also the form of the divergence of a current (we have only included the lowest-order term), plus a nonconserved contribution $-vm$ due to the incoming current of particles that tends to reduce the value of the order parameter. The lowest order coupling to the height variable in equation (4) is of the form $\nabla^2(m\nabla^2 h)$, which is irrelevant. In contrast to the vapor deposition case, the parameter v can never become negative, making a term in m^3 unnecessary. Instead, the tendency towards phase separation is locally captured by $K < 0$, which is the main focus of the work by Léonard and Desai [10,11], and of Atzmon et al. [5] (the latter study does not include the height profile). A change in the sign of K marks the onset of phase separation in models of conserved dynamics. Higher order terms, such $\nabla^4 m$ or $\nabla^2 m^3$ which are included by other authors, are then needed for the stability of short wavelength fluctuations, and may also affect the precise shape of the order parameter profile within domains. Such terms are irrelevant to considerations of the long wavelength behavior of equation (4), since in this case instabilities can only persists up to a length scale of the order $\sqrt{K/v}$, set by the current of incoming particles. Since higher temperatures and deposition rates favor mixing, it is likely that K eventually becomes positive as these parameters are increased. If the substrate dimension is $d = 1$ (or is effectively $d = 1$ because diffusion proceeds along a preferred direction) the coarse-grained value of K must be positive, as the dynamics are then similar to a 1-dimensional Ising model, which cannot have an ordered phase. For this reason, the choice of $K < 0$ in [10,11] does not capture the long wavelength behavior of the system.

The main focus of the next two sections is on the model for vapor deposition, equations (1, 2), and we discuss equations (3, 4) only briefly in connection with the RG calculation. Our analysis of the models will concentrate on the scaling behavior of the height profile and of the order parameter. On sufficiently large length scales, height profiles of growing interfaces are usually characterized by a scaling form

$$\langle [h(\mathbf{x},t) - h(\mathbf{x}',t')]^2 \rangle \sim |\mathbf{x}-\mathbf{x}'|^{2\chi} g\left(\frac{|t-t'|}{|\mathbf{x}-\mathbf{x}'|^{z_h}}\right), \tag{5}$$

where χ is the roughness exponent, and z_h is a dynamical scaling exponent. The values of the exponents depend on the underlying growth model, and one of our objectives is to find out how they are affected by the coupling to the order parameter dynamics.

The scaling of the order parameter is different along the growth direction and perpendicular to it. In contrast to the height variable, the order parameter is unlikely to be exactly at a fixed point, and for this reason we include a correlation length ξ. We also have to allow for the possibility that the height and the order parameter dynamics have different dynamical critical exponents z_h and z_m. The scaling laws for the order parameter then read

$$\begin{aligned} G_m^{(x)}(\mathbf{x}-\mathbf{x}') &\equiv \langle m(\mathbf{x},t)m(\mathbf{x}',t)\rangle - \langle m\rangle^2 \\ &= |\mathbf{x}-\mathbf{x}'|^{\eta-1} g_m^{\perp}(|\mathbf{x}-\mathbf{x}'|/\xi) \\ G_m^{(t)}(t-t') &\equiv \langle m(\mathbf{x},t)m(\mathbf{x},t')\rangle - \langle m\rangle^2 \\ &= |t-t'|^{(\eta-1)/z_m} g_m^{\parallel}(|t-t'|/\xi^{z_m})\,. \end{aligned} \tag{6}$$

3 Renormalization group analysis

Let us now renormalize the equations of motion, equations (1, 2), and search for fixed points that are accessible by perturbation theory. Inserting the equations of motion in the Gaussian probability distribution of the noise

$$W[\zeta_h,\zeta_m] \propto \exp\left\{-\int d^dx\; dt\left[\frac{\zeta_h(\mathbf{x},t)^2}{4D_h} + \frac{\zeta_m(\mathbf{x},t)^2}{4D_m}\right]\right\}, \tag{7}$$

and introducing auxiliary fields $\tilde{m}$ and $\tilde{h}$, we obtain the weight of a given space-time configuration $[h(\mathbf{x},t), m(\mathbf{x},t)]$ [13]

$$W[h,m] \propto \int \mathcal{D}[i\tilde{h}] \int \mathcal{D}[i\tilde{m}] \exp\left\{\mathcal{J}[\tilde{h},h,\tilde{m},m]\right\},$$

with the dynamical functional

$$\begin{aligned} \mathcal{J}\left[\tilde{h},h,\tilde{m},m\right] = \int d^dx \int dt \Bigg\{ & D_h\tilde{h}\tilde{h} - \tilde{h} \\ & \times \left[\frac{\partial h}{\partial t} - \nu\nabla^2 h - \frac{\lambda}{2}(\nabla h)^2 - \frac{\alpha}{2}m^2\right] \\ & + D_m\tilde{m}\tilde{m} - \tilde{m} \qquad (8) \\ & \times \Big[\frac{\partial m}{\partial t} - K(\nabla^2 m - rm - um^3) \\ & - a\nabla h\cdot\nabla m - bm\nabla^2 h - \frac{c}{2}m(\nabla h)^2\Big]\Bigg\}. \end{aligned} \tag{9}$$

The dynamical functional $\mathcal{J}$ plays the same role in dynamical RG as the Hamiltonian in statics. The bare

Table 1. Bare dimensions d_0, scaling dimensions d_g at the Gaussian fixed point, and scaling dimensions d_α between 4 and 6 dimensions of all the couplings.

coupling	d_0	d_g	d_α
D_m	$z-d-2\zeta$	0	0
K	$z-2$	0	0
r	2	2	2
u	$2+2\zeta$	$4-d$	$4-d$
a	$z-2+\chi$	$(2-d)/2$	$4-d$
b	$z-2+\chi$	$(2-d)/2$	$4-d$
c	$z-2+2\chi$	$2-d$	$2(4-d)$
D_h	$z-d-2\chi$	0	$d-6$
ν	$z-2$	0	0
λ	$z-2+\chi$	$(2-d)/2$	$4-d$
α	$2\zeta-\chi+z$	$(6-d)/2$	0
β	$2\zeta-\chi+z-2$	$(2-d)/2$	

propagators of this model are

$$G_0^h(\mathbf{k},t) \equiv \langle \tilde{h}(-\mathbf{k},t)h(\mathbf{k},t)\rangle_0 = \theta(t)e^{-\nu k^2 t}, \quad (10)$$

$$C_0^h(\mathbf{k},t) \equiv \langle h(-\mathbf{k},t)h(\mathbf{k},t)\rangle_0 = \frac{D_h e^{-\nu k^2|t|}}{\nu k^2}, \quad (11)$$

$$G_0^m(\mathbf{k},t) \equiv \langle \tilde{m}(-\mathbf{k},t)m(\mathbf{k},t)\rangle_0 = \theta(t)e^{-K(r+k^2)t}, \quad (12)$$

$$C_0^m(\mathbf{k},t) \equiv \langle m(-\mathbf{k},t)m(\mathbf{k},t)\rangle_0 = \frac{D_m e^{-K(r+k^2)|t|}}{K(r+k^2)}, \quad (13)$$

and the interaction vertices are obtained from the higher-order terms in J. In the diagrams below, h and $\tilde{h}$ are represented by straight and wiggly lines respectively. Lines for the order parameter m are represented the same way, with an additional short dash perpendicular to the propagator.

The bare dimensions d_0 of the couplings are obtained by rescaling space, time, height, and order parameter according to $x = bx'$, $t = b^z t'$, $h = b^\chi h'$, $\tilde{h} = b^{\tilde{\chi}}\tilde{h}'$, $m = b^\zeta m'$, $\tilde{m} = b^{\tilde{\zeta}}\tilde{m}'$, and by requiring invariance of the Gaussian part of $\mathcal{J}$ under such rescaling. (The scaling dimension ζ of the order parameter is related to the exponent η defined in Eq. (6) via $\zeta = (\eta-1)/2$.) The results are listed in Table 1. In the following, we analyze the scaling behavior resulting from an RG analysis as function of the spatial dimension d.

3.1 Dimensions d > 6

In sufficiently high dimensions, the Gaussian fixed point, which is characterized by uncoupled, linear Langevin equations is stable with respect to the higher-order terms. The condition of scale invariance of the linear Langevin equations leads to $z = 2$ and $\chi = \zeta = (2-d)/2$, and to the scaling dimensions d_g listed in the third column of Table 1. In dimensions $d > 6$, all nonlinear couplings are irrelevant. The surface is smooth, and the order parameter goes through a classical phase transition.

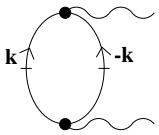

Fig. 1. The diagram renormalizing D_h. The lines with a small bar represent the order parameter propagators, while lines without this bar belong to the height variable. Wiggled lines stand for $\tilde{h}$ and $\tilde{m}$, and smooth lines for h and m.

3.2 Dimensions 4 < d < 6

Below $d = 6$, the coupling α becomes relevant. The Gaussian fixed point still exists, but becomes unstable. A new stable fixed point with a nonzero value of α emerges. Whenever nonlinear terms cannot be neglected, the couplings change under rescaling not only according to their bare dimensions, but also according to those contributions that are generated under renormalization. Renormalization of this model is done by first integrating over the large wave vectors $\Lambda/b < k < \Lambda$, where Λ is the wave vector cutoff, and the scaling factor b is larger than 1. Next, the system is rescaled to the original size by introducing new variables $k' = bk$, $t' = t/b^z$. This procedure involves an expansion of $e^{\mathcal{J}}$ in the couplings. In this way, the coupling α generates a contribution to D_h, which is graphically represented by the diagram in Figure 1. Evaluation of this diagram gives a contribution to D_h of

$$B = \frac{\alpha^2 D_m^2}{2K^2} \int_{\Lambda/b<|\mathbf{k}|<\Lambda} d^d k \int_0^\infty dt \frac{e^{-2K(r+k^2)|t|}}{(r+k^2)^2} = \frac{\alpha^2 D_m^2 K_d \Lambda^{d-6}(1-b^{6-d})}{4K^3(d-6)},$$

where K_d is the surface of the d-dimensional unit sphere, divided by $(2\pi)^d$. We have also set $r = 0$, assuming that the order parameter is exactly at its critical point. The renormalized value of this parameter is thus

$$D_h' = b^{z-d-2\chi}[D_h + B].$$

Setting $b = 1 + dl$, we obtain the flow equation

$$\frac{dD_h}{dl} = -D_h(d+2\chi-z) + \frac{\alpha^2 D_m^2 K_d \Lambda^{d-6}}{4K^3}. \quad (14)$$

The exponents z and ζ are fixed at the values $z = 2$ and $\zeta = (2-d)/2$, since the renormalization of the parameters ν, K, D_m does not obtain any anomalous contributions from diagrams. The condition that α has a nonzero fixed point leads to $\chi = 4-d$. With these values of the exponents, the condition that D_h is invariant under rescaling leads to the fixed point value of D_h

$$D_h = \frac{\alpha^2 D_m^2 K_d \Lambda^{d-6}}{4K^3(6-d)}. \quad (15)$$

This fixed point, where α is the only nonzero coupling is stable between 4 and 6 dimensions. The scaling dimensions

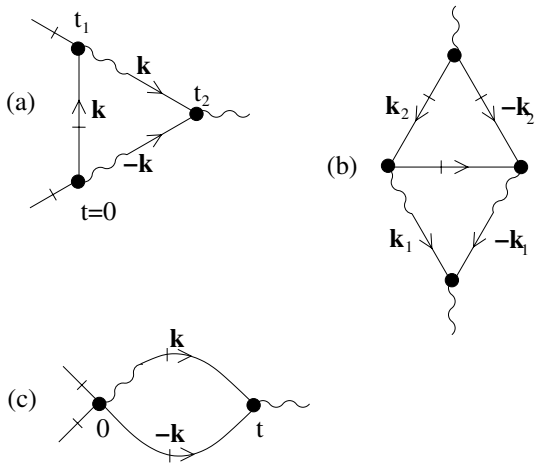

Fig. 2. The diagrams to be considered near $d = 4$ dimensions.

of the other couplings are given in the right-hand column of Table 1.

Note that for $4 < d < 6$, the term αm^2 can be regarded as a correlated noise acting on the surface height. This correlated noise is more relevant than the white noise, and increases the value of the roughness exponent χ from $(2-d)/2$ to $4-d$. As this value is still negative, the surface is flat at this fixed point.

3.3 Dimensions d $\simeq$ 4

Below $d = 4$ dimensions, the flat phase becomes unstable, because the roughness exponent becomes positive, and the coupling λ obtains a positive scaling dimension. In $d = 4 + \epsilon$ dimensions (with $|\epsilon|$ small), we can therefore expect a fixed point where λ (or a power of λ) is of the order of ϵ. In order to find this fixed point, let us first assume that there is no feedback from the height to the order parameter ($a = b = c = 0$), and then take into account all terms of the lowest order in λ.

As shown in Figures 2a and b, there are two diagrams that contain one λ vertex. Diagram (a) makes a contribution to $\alpha/2$ equal to

$$\begin{aligned} A =& \alpha^2\lambda \int\limits_{\Lambda/b<|\mathbf{k}|<\Lambda} d^dk \int\limits_0^\infty dt_1 \int\limits_{t_1}^\infty dt_2 \\ & \times \frac{k^2 D_m e^{-\nu k^2(2t_2-t_1)-K(r+k^2)t_1}}{K(r+k^2)} \\ =& \frac{\alpha^2\lambda D_m K_4 \Lambda^\epsilon dl}{2K\nu(K+\nu)}, \end{aligned}$$

which is a correction of order $\lambda\alpha^2$. Figure 2b is a correction to D_h of order $\lambda\alpha^3$. Since it modifies the flow equation (14) for D_h only to order ϵ, it need not be evaluated. Furthermore, equation (2) describes for $a = b = c = 0$ the relaxational dynamics of an order parameter in the universality class of the Ising model, which is known to have a non-trivial stable fixed point for $D_m u/K = -K_4\epsilon/9 + \mathcal{O}(\epsilon^2)$ below 4 dimensions, and with r of the order of ϵ [14]. This means that we have to take into account additionally diagram 2c, which makes for $d < 4$ a contribution

$$C = -3\alpha u K \int\limits_{\Lambda/b<|\mathbf{k}|<\Lambda} d^dk \int\limits_0^\infty dt \frac{D_m e^{-2K(r+k^2)t}}{K(r+k^2)} = \frac{\epsilon\alpha dl}{6}$$

to $\alpha/2$, which is of order ϵ. In evaluating this expression, we have inserted the above-mentioned fixed point value of $D_m u/K$ and have set $r = 0$, considering only the leading contribution in an expansion in ϵ.

Taking all these results together, we obtain the following set of flow equations to order ϵ:

$$\begin{aligned} \frac{dD_m}{dl} &= D_m(z-d-2\zeta)\,; \\ \frac{dK}{dl} &= K(z-2)\,; \\ \frac{d\nu}{dl} &= \nu(z-2)\,; \\ \frac{d\lambda}{dl} &= \lambda(z-2+\chi)\,; \\ \frac{dD_h}{dl} &= -D_h(d+2\chi-z) + \frac{\alpha^2 D_m^2 K_d \Lambda^{d-6}}{4K^3} + \mathcal{O}(\epsilon)\,; \\ \frac{d\alpha}{dl} &= \alpha\left[2\zeta-\chi+z+\frac{\theta(-\epsilon)\epsilon}{3}+\frac{\alpha\lambda D_m K_4}{K\nu(K+\nu)}\right]. \end{aligned} \quad (16)$$

From the flow equations for K, ν and D_m, we obtain again the fixed point condition $z = 2$ and $\zeta = (2-d)/2$. For $\epsilon > 0$, the fixed point $\lambda = 0$ is stable, and we have a negative roughness exponent $\chi = 4 - d$, as before. For $\epsilon < 0$, the fixed point $\lambda = 0$ is unstable, with the roughness exponent χ modified due to diagram (c) in Figure 2. For $\lambda = 0$ and $\epsilon < 0$, equation (16) reduces to

$$\frac{d\alpha}{dl} = \alpha\left(-\epsilon-\chi+\frac{\epsilon}{3}\right) = \alpha\left(-\chi-\frac{2\epsilon}{3}\right)$$

leading to $\chi = 2(4-d)/3$.

Let us next discuss the fixed point with $\lambda \neq 0$. A nonzero λ requires $\chi = 0$. The combination $\alpha\lambda$ then acts as an effective coupling, and equation (16) has a non-trivial fixed point at

$$\alpha\lambda = \epsilon\frac{K\nu(K+\nu)}{D_m K_4} + \mathcal{O}(\epsilon^2), \quad (17)$$

for $\epsilon > 0$ and a fixed point

$$\lambda\alpha = \epsilon\frac{2K\nu(K+\nu)}{3D_m K_4} + \mathcal{O}(\epsilon^2), \quad (18)$$

for $\epsilon < 0$. The couplings a, b, and c have scaling dimension zero (to order ϵ) and are thus marginal at this fixed point. Determination of their marginal relevance or irrelevance requires evaluation of higher order terms in ϵ, which was not attempted in this paper. For $\epsilon < 0$, the fixed point is *stable* as indicated by the flows sketched in Figure 3. We expect it to correspond to a rough phase, with the

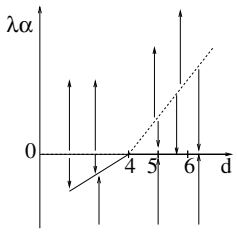

Fig. 3. The flow of the coupling $\lambda\alpha$ near $d = 4$ dimensions. The arrows indicate the direction of the RG flow of $\lambda\alpha$. The dashed line marks unstable fixed points, and the solid line stable fixed points.

roughness exponent $\chi = 0$, possibly receiving corrections in higher order in ϵ. For $\epsilon > 0$, the fixed point can be interpreted as describing a roughening transition. The fixed point is unstable (see Fig. 3), with flows to either a flat phase (if the initial λ value is smaller than the fixed point value) or to a rough phase, which is not accessible by perturbation theory. Compared to a system that is described by the height variable alone, without a coupling to critical order parameter fluctuations [9], the lower critical dimension for the roughening transition is increased, at criticality of order parameter fluctuations, from 2 to 4. We thus have found that the coupling to the critical order parameter fluctuations changes the scaling behavior of the height variable below 6 dimensions, and that it increases the lower critical dimension for the roughening transition from 2 to 4. Studying the influence of the surface roughness on the critical order parameter fluctuations near 4 dimensions was not possible to us within perturbation theory. To order ϵ, the parameters a, b, c are marginal, and to higher orders in ϵ the number of diagrams becomes large. Furthermore, it is not clear whether further fixed points except those discussed by us are at all accessible by perturbation theory.

In the case of the conserved Langevin equations (3, 4) proposed for MBE growth, the mutual effects between height and order parameter are much weaker. The Gaussian fixed point is stable above $d = 2$ dimensions. Below $d = 2$, the coupling β becomes relevant. If $K > 0$ and v is small ($v \ll \Lambda^2/K$), the diffusion of the order parameter on the surface affects the height profile. Performing an analysis analogous to the one above near 6 dimensions (where α was the relevant coupling), we find a stable fixed point in $d = 2 - \epsilon$ with $\beta^2 = D_h\kappa^3\pi\epsilon/2D_m^2 + \mathcal{O}(\epsilon^2)$ and $\chi = 2 - d$. (Without coupling to the order parameter, there is a smaller roughness exponent of $\chi = (2 - d)/2$.) For negative K, there can be other interesting (non critical) effects, as mentioned before.

4 Computer simulations

While the RG gives information about scaling behavior in high dimensions (4 and higher), computer simulations are particularly efficient in low dimensions. In this section, we present results from simulations in 1+1 dimension. Rather than discretizing equations (1–2) and integrating them numerically, we perform numerical studies of a "brick wall" restricted solid-on-solid model (see Fig. 4). Since this model shares the same symmetries and conservation laws as the Langevin equations, it should share the same universality properties.

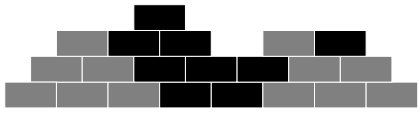

Fig. 4. The "brick wall" model used in the simulations.

Starting from a flat surface, particles are added such that no overhangs are formed, and with the center of each particle atop the edge of two particles in the layer below. We use two types of particles, A and B (black and grey in the figure). The probability for adding a particle to a given surface site, and the rule for choosing its color, depend on the local neighborhood. Since growth is slower on slopes, these growth rules correspond to $\lambda < 0$ [16,17].

When A (B) particles are more likely to be added to A dominated regions (B), the particles tend to phase separate and form domains. In this case, the order parameter correlation length ξ is of the order of the average domain width. By changing the growth rules, it is possible to study cases in which some (or all) of the couplings a, b, c, and α vanish, and thus to gain a more complete picture of the different ways in which the height and the order parameter influence each other.

When all the couplings between the order parameter and the height vanish ($a = b = c = \alpha = 0$), the well-known critical exponents $z_h = 3/2$ and $\chi = 1/2$ of the KPZ equation [9,15], and $z_m = 2$ and $\eta = 1$ of the Glauber model [18] are recovered. This situation is implemented in the following way: A surface site is chosen at random, and a particle is added if it does not generate overhangs. Its color is then chosen depending on the colors of its two neighbors in the layer below. If both neighbors have the same color, the newly added particle takes this color with probability $1 - p$, and the other color with probability p (where p is much smaller than 1). If the two neighbors have different colors, the new particle takes either color with probability 1/2. Neighbors within the same layer are not considered. As discussed in reference [12], these growth rules lead to an order parameter correlation length $\xi \sim 1/\sqrt{p}$ as $p \to 0$.

Here, we want to focus on the more interesting situations where either α or a, b, c (or all of them) are nonzero. In the first case presented below, the order parameter affects the height variable, but is not influenced by it. In the second case, the height profile affects the order parameter dynamics, but not vice versa. One would expect that in the first case the order parameter imposes its dynamical exponent $z = 2$ on the dynamics of the height profile, and that in the second case the height profile imposes its exponent $z = 3/2$ on the order parameter. This latter is, however, not the case for $a/\lambda < 0$, and we shall see that z_m is nonuniversal in this case. In the fully coupled case with α, a, b, and c not equal to zero, we find $z = 2$ or $z = 3/2$,

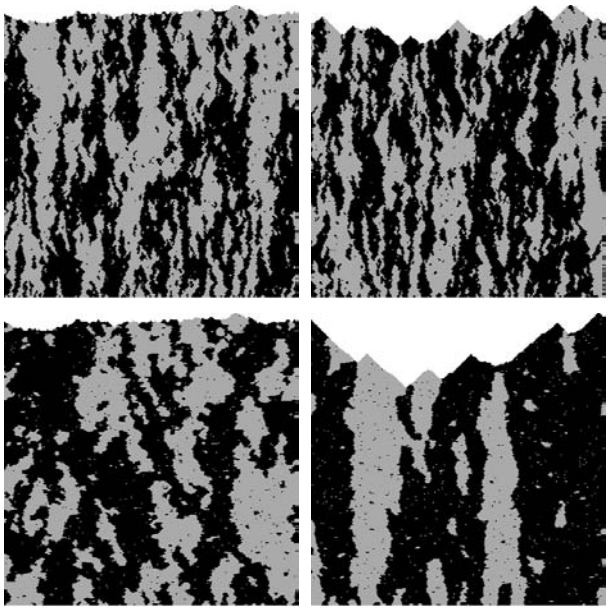

Fig. 5. Snapshot of the last 400 layer of simulations, for $L = 200$ sites and $p = 1/90$. Top left: The decoupled case $\alpha = a = b = c = 0$. Top right: The case $\alpha > 0$ and $a = b = c = 0$ for $r = 1/15$. Bottom left: The case $\alpha = 0$ and $a > 0$. Bottom right: The case $\alpha > 0$ and $a > 0$ for $r = 1/15$. Note that the profiles in the left figures are the same since we used the same random numbers.

depending on the sign of $(\lambda\alpha)$. Some of these results were already reported in reference [12].

4.1 Growth influenced by independent phase ordering ($\alpha \neq 0$, a, b, c = 0)

The situation $\alpha > 0$ ($\alpha < 0$) is implemented by updating sites on top of particles of different colors less (more) often by a factor $r < 1$ ($r > 1$) compared to sites above particles of the same color. If the color of the new particle depends only on the neighbors in the layer below, the order parameter is not affected by the height variable, and its dynamics is still the same as that of an Ising model, with $z_m = 2$.

We first discuss the case $\alpha > 0$: Because growth is slower at domain boundaries than within domains, the domain boundaries sit preferentially at the local minima of the height profile, with a mound over each domain. (see Fig. 5). This implies that the surface roughness exponent is $\chi = 1$ on length scales up to ξ. Changes in the height profile on this scale result from domain wall diffusion, and the dynamical exponent is therefore $z_h = 2$. On length scales much larger than ξ, the average order parameter is zero, implying that KPZ exponents of $\chi = 1/2$ and $z_h = 3/2$ are regained. The crossover in the roughness is described by a scaling form

$$\langle [h(x,t) - h(x',t)]^2 \rangle = |x - x'|^2 g\left(\frac{|x - x'|}{\xi}\right),$$

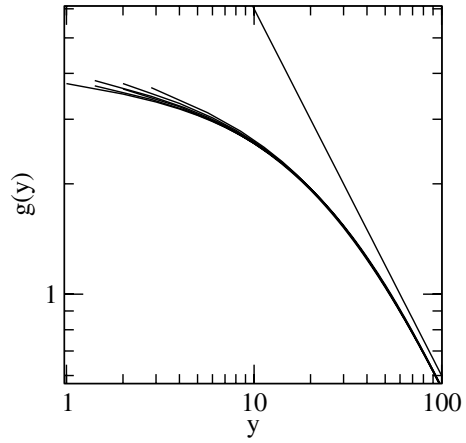

Fig. 6. The scaling function $g(y)$, obtained for $L = 2048$ by collapsing data for $p^{-1} = 320$, 640, 1280, and 2560. For r, the values 0.05 and 0.025 were used. The dashed line is a power law $\propto 1/y$.

with a constant $g(y)$ for $y \ll 1$, and $g(y) \sim 1/y$ for $y \gg 1$. Figure 6 shows our simulation results for $g(y)$, obtained by the data collapse of $\langle [h(x,t) - h(x',t)]^2 \rangle / |x - x'|^2$ versus $|x - x'|\sqrt{p}$, for different values of p. The curves for the two different values of r differed only slightly, and were collapsed by multiplying the curves for $r = 0.05$ by a factor of 1.06. The scaling collapse is compatible with $g(y) \sim 1/y$ for large y, and $g(y) \rightarrow$constant, for small y.

For $\alpha < 0$, growth occurs with a larger probability at domain boundaries. Therefore, domain boundaries sit at local maxima. However, further away from the domain boundaries, their effect is not felt, and we find $\chi = 1/2$ and $z_h = 3/2$, just as in the case $\alpha = 0$.

A simplified version of the situation discussed in this subsection was investigated by Wolf and Tang [20], who considered a growing surface with growth slowed down or accelerated at equally spaced fixed positions. The surface can respond on larger scales to the inhomogeneity at these positions only when $\lambda\alpha < 0$. Furthermore, the situation of one single domain wall with decelerated or accelerated growth can be mapped on the asymmetric exclusion process with one second-class particle that moves slower or faster than the other particles [21].

4.2 Phase ordering influenced by independent growth ($\alpha = 0$; a, b, c $\neq 0$)

The situation $\alpha = 0$ is implemented by choosing $r = 1$, i.e., adding a particle at each possible site with the same probability, irrespective of the color of its neighbors. To mimic the influence of surface roughness on the order parameter (nonzero a, b, or c in Eqs. (2)), the color of a newly added particle is made dependent not only on those of its two neighbors in the layer below, but also on the colors of its two nearest neighbors on the same layer, if these sites are already occupied. With probability $1 - p$, the newly added particle takes the color of the majority of its 2, 3, or 4 neighbors, and with probability p it assumes the

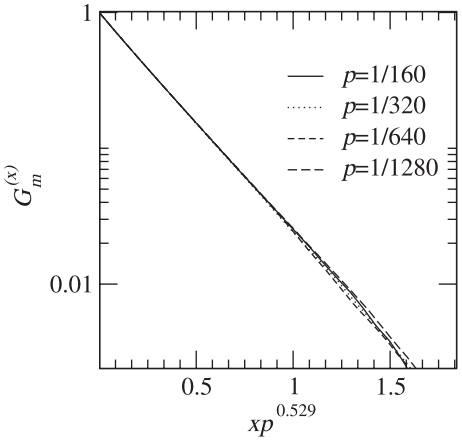

Fig. 7. Scaling collapse of the correlation functions $G_m^{(x)}$ for $q = 0.25$ and different values of p.

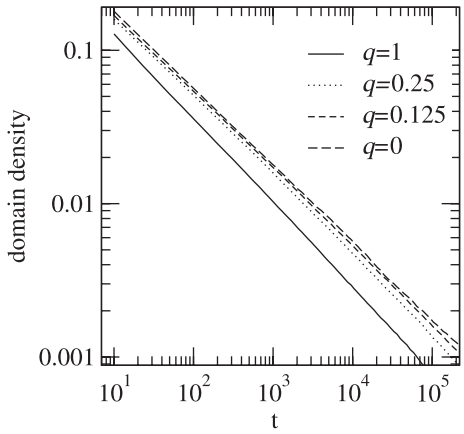

Fig. 8. Domain density (i.e., number of domains, divided by the system size) as a function of time for $L = 16384$, averaged over 100 samples, for 4 different values of q. The curves are well fitted by power laws of the form t^{-1/z_m} with the exponents z_m=1.8, 1.89, 1.96, 2.0.

opposite color. If there is a tie, the color is chosen at random with equal probability. Since the neighbor on the hillside of a site is more likely to be occupied than the one on the valley side, with this rule domain walls are driven downhill, corresponding to $a > 0$ in equation (2). Also, domains on hilltops can expand more easily than those on slopes or in valleys, suggesting a value of $b > 0$.

We reported already in reference [12] that the dynamical critical exponent z_m associated with the order parameter has a nontrivial dynamic exponent of $z_m \simeq 1.85$, and not the value $z_m = 1.5$, which may be expected if the walls follow the surface fluctuations. A potential explanation was provided in reference [19] in connection with the dynamics of a single domain wall riding on a growing surface. The growth rules for the surface imply that sequences of brick addition usually proceed from local minima in the uphill direction, since the addition of a brick generates a potential growth site (where a brick can be added without generating overhangs) at the nearest uphill position. The walls that try to slide downhill are therefore faced with an upward avalanche of growth mounds of different sizes that hamper their downhill motion.

The exponent z_m is not only nontrivial, but also nonuniversal and depends on the value of a. A change in a can be implemented in the computer simulations by taking into account neighbors within the same layer as the site being updated with a probability q smaller than 1. Using the above-mentioned rules and values of $q = 1$, 0.25, 0.125, 0, we find $z_m = 1.8$, 1.89, 1.96, 2.0. The difference from the value for $q = 1$ reported in reference [12] stems from the fact that in that paper we had inadvertently assigned to neighbors within the same layer a double weight – thus illustrating once more the nonuniversality of the value of z_m. Each of these values was evaluated in two independent ways, in order to confirm its stability and parameter dependence. The first was a collapse of the correlation function $G_m^{(x)}(x)$, as shown in Figure 7. Since p sets the inverse time scale, the scaling variable is xp^{1/z_m}, yielding the value of z_m. The second method was a domain coarsening simulation, following a quench from $p = 0.5$ to $p = 0$. Figure 8 shows the number of domains, divided by the system size, as function of time for different values of q. Both methods yield the same values for the exponent z_m, thus supporting the conjecture that the exponent is indeed nonuniversal. The alternative scenario, a very slow crossover, would most likely not yield the same values of the apparent exponents for both methods.

Equations (1–2) allow also for the possibility of $a < 0$. This would imply that domain walls move uphill and that identical neighbors in the same layer have a positive interaction energy, in contrast to neighbors in different layers. Although this is an implausible physical situation, it is nevertheless of some theoretical interest. For $a = \lambda$ and $c = 0$, the invariance under the transformation $x' = x - \lambda\epsilon t$ and $h' = h + \epsilon x$ (with a small ϵ) of the KPZ equation holds also for equation (2). This invariance corresponds to the Galilean invariance of Burger's equation. It implies that the order parameter dynamics are governed by the same time scale as the height variable, i.e., $z_m = z_h$. Implementing the case $a < 0$ in our simulations, we indeed find $z_m = 1.5$, suggesting that the Galilean invariant fixed point is the only attractive fixed point in this domain of parameters.

4.3 Mutual couplings (α, a, b, c $\neq$ 0)

When all couplings are different from zero, the probability for adding a particle at a given site and the choice of the particle color depend on the local neighborhood. The simulation parameter q is positive, and r is different from 1.

For $\alpha > 0$, we find $z_m = 2$ irrespective of the values of a, b, and c. As particles are added to domain boundaries with a smaller probability than within domains, domain boundaries sit at local minima most of the time. Therefore they perform a random walk even when $a \neq 0$. Over each domain there is a mound, implying that $\chi = 1$ on length scales up to ξ. Changes in the height profile on this scale result from domain wall diffusion, and the dynamic

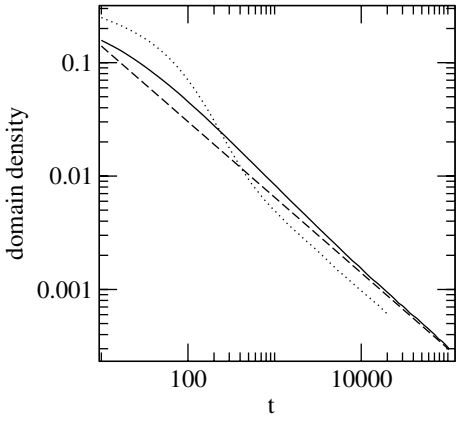

Fig. 9. Domain density (i.e., number of domains, divided by the system size) as a function of time for $a\lambda < 0$ and $L = 16384$, averaged over 100 samples, for $q = 1$ and $r = 5$ (solid line). The dashed line is a power law with an exponent $-2/3$, corresponding to $z_m = 1.5$. The dotted curve shows the corresponding simulation result with positive $a\lambda$.

exponent is therefore $z_h = 2$. On length scales much larger than ξ, the average order parameter is zero, and KPZ exponents of $\chi = 1/2$ and $z_h = 3/2$ are regained.

For $\alpha < 0$, particles are added rapidly on domain boundaries, and domain walls can therefore not be trapped in local height minima. For the case $a\lambda > 0$, where domain walls tend to move uphill, we therefore expect that the situation $\alpha < 0$ is similar to the case $\alpha = 0$, for which we found $z_m = z_h = 3/2$. This means that the abovementioned Galilean-invariant fixed point remains applicable to $\alpha < 0$. The simulation results shown in Figure 9 confirm this expectation. For the case $a\lambda < 0$ and $\alpha = 0$, we have argued above that the downhill motion of domain walls is hampered by an upward avalanche of growth mounds, which cause the walls to be temporarily stuck in local minima, leading to a nonuniversal exponent z_m. Now, for $\alpha < 0$ and $a\lambda < 0$, we find in our simulations that the dynamical critical exponent z_m is identical to $z_h = 1.5$, implying that the downhill motion of the domain walls is not hampered any more but that the domain walls can follow the height fluctuations. Figure 9 shows the results of a domain coarsening simulation for the parameters $q = 1$ and $r = 5$. For comparison, simulation results for positive $a\lambda$ (and otherwise the same parameter values) are also shown. One can see that the exponent z_m is indeed the same in both situations. To summarize, we find that for $\alpha < 0$ the height profile imposes its critical behavior on the order parameter fluctuations, while in the opposite case, $\alpha > 0$, the domain wall diffusion imposes a dynamical exponent $z = 2$ on the system.

4.4 Comparison to analytical results

It is interesting to compare the results of the computer simulations with the admittedly limited results of the RG analysis presented in the previous section.

Let us start from our last result that for $\alpha\lambda > 0$ the height profile imposes its critical behavior on the order parameter, while the reverse is true for $\alpha\lambda < 0$. The RG up to order $\epsilon = 4 - d$ showed that for $\alpha\lambda < 0$ the fixed point is accessible perturbatively, with $z = 2$ to order ϵ. It is striking that this result holds also in $1 + 1$ dimension. For $\alpha\lambda > 0$, the RG flow runs away to infinity, suggesting the existence of a strong coupling fixed point. The critical behavior corresponding to this fixed point was found in our simulations in 1+1 dimension to be the same as that of the KPZ equation, with $z = 3/2$. If this result is not particular to 1+1 dimension, it suggests that a positive $\alpha\lambda > 0$ might be irrelevant at the KPZ strong coupling fixed point. However, this conclusion can not be tested via by perturbative RG analysis.

Up to order ϵ of the RG analysis, the parameters a, b, c are marginal. It appears from our simulations that these three coupling indeed do not modify the critical behavior as long as $\alpha \neq 0$, suggesting that these parameters are marginally irrelevant.

For $\alpha = 0$, the critical behavior of the height profile is given by the KPZ equation, and it has a stable fixed point at $\lambda = 0$ in which the dimension of h is $(2 - d)/2 < 0$. Thus at the weak coupling fixed point, a, b, and c are irrelevant in four dimensions and the Ising fixed point is not modified by coupling to the height parameter. However, the RG analysis cannot predict the critical behavior of the coupled system in the rough phase, which is characterized by a strong coupling fixed point. Nevertheless, we could argue that there exists a Galilean-invariant fixed point when $a\lambda > 0$, where the height profile imposes its dynamical critical exponent on the order parameter. The result $z_m = 2$ in 1+1 dimensions was confirmed by our computer simulations, suggesting a larger domain of parameter space where such scalings apply.

The only case for which we have no analytical prediction is when $\alpha = 0$, and $\lambda a < 0$, where the computer simulations reveal nonuniversal behavior.

5 Relation to passive scalar advection and drifting polymers

There is a close connection between the model studied in this paper and other coupled nonequilibrium systems. One such system is obtained when we regard domain walls as "particles" that ride on the growing surface. With the substitution $\nabla m = \rho$, we obtain for $u = b = c = 0$ the following equation for ρ:

$$\frac{\partial \rho}{\partial t} = \kappa \nabla^2 \rho + a \nabla(\rho \nabla h) + \zeta_\rho(\mathbf{x}, t), \tag{19}$$

with a conserved noise ζ_ρ. Without the noise term this equation is the Fokker Planck equation corresponding to the Langevin equation

$$\frac{d\mathbf{x}}{dt} = a \nabla h + \zeta_x(t)\,. \tag{20}$$

If we assume that the particles do not interact with each other, the Fokker Planck equation, combined with a noise term, describes the time evolution of the particle density.

If we require additionally that there is no effect of the particles on the growing interface, the coupling α vanishes, too. The substitution $\nabla h = \boldsymbol{v}$ then turns the KPZ equation into a randomly stirred Burger's equation, and equation (20) becomes the equation of motion of a particle advected by the flow. This model was studied in detail in reference [19]. Just as for the model described in this paper, the scaling behavior of the advected particles is fundamentally different in the two cases $a/\lambda > 0$ and $a/\lambda < 0$. In the first case, the system has a Galilean invariant fixed point, and particle diffusion is characterized by a dynamical critical exponent $z_\rho = 3/2$ in one dimension, while this exponent is larger than 3/2 and nonuniversal in the other case.

Finally, equations (1–2) with $a = b$ and $c = r = u = 0$, but with $\alpha \neq 0$, can be mapped on the equations used to describe the dynamics of a stretched string moving in a random medium [22]. If the string is stretched in the x-direction, and if it moves in the h-direction, the configuration of a string embedded in 3 dimensions can be characterized by the coordinates $h(x)$ and $h_\perp(x)$. Assuming that the evolution of the line is dissipative and local, the equations of motion then are our equations (1–2) with the replacement $m = \partial_x h_\perp$ and with ζ_m replaced with a conserved noise $\partial_x \zeta_m$. Apart from the Galilean-invariant fixed point, this set of equations has a fixed point where a fluctuation-dissipation relation is satisfied (i.e. where a stationary solution of the Fokker-Planck-equation can be written down). This fixed point corresponds in our notation to the situation $\alpha = Ka/\nu$. (For a general discussion of equations the stationary solutions of which can be calculated, see Ref. [24]).

6 Conclusions

In summary, the interplay between surface roughening and phase separation leads to a variety of novel critical scaling behaviors. At one extreme, the height profile adapts to the dynamics of critical domain ordering. At the other extreme, the dynamics of the domain walls follow the height fluctuations. For a third range of parameter values, the dynamics of domain wall motion is influenced by the roughness, but exhibits nontrivial and nonuniversal scaling behaviors.

Several generalizations of the model presented in this paper are possible. For example, as discussed in reference [23], one can consider the situation where the symmetry breaking involves a continuous, rather than an Ising-like order parameter. Such a situation applies to the deposition of spins that can realign on the surface but are frozen in the bulk, or to orientational symmetry breaking in the plane during crystal growth. Another generalization would be the inclusion of elastic forces, which are often present during the growth of composite films (see Ref. [24]). Furthermore, one could consider phase transitions where the different types of molecules order on sublattices instead of phase separating.

Finally, there exist growth situations where one type of particles is magnetic. In addition to a ordering or phase separation transition which occurs at the surfaces, there is in this case also a magnetic phase transition, which occurs in the bulk. This combination of two-dimensional and three-dimensional phase transitions is particularly challenging for a theoretical analysis, and it leads to interesting experimental results [25].

This work was supported by the Deutsche Forschungsgemeinschaft (DFG) under Contract No Dr300-2/1 (BD), and by the National Science Foundation grant DMR-01-18213 (MK).

References

1. T.L. McDevitt, S. Mahajan, D.E. Loughlin, W.A. Bonner, V.G. Keramidas, Phys. Rev. B **45**, 6614 (1992)
2. C.D. Adams, M. Atzmon, Y.-T. Cheng, D.J. Srolovitz, J. Mater. Res. **72**, 653 (1992)
3. Y. Bar-Yam, D. Kandel, E. Domany, Phys. Rev. B **41**, 12869 (1990)
4. B. Drossel, M. Kardar, Phys. Rev. E **55**, 5026 (1997)
5. M. Atzmon, D.A. Kessler, D.J. Srolovitz, J. Appl. Phys. **72**, 442 (1992)
6. C.D. Adams, D.J. Srolovitz, M. Atzmon, J. Appl. Phys. **74**, 1707 (1993)
7. M. Ausloos, N. Vandewalle, R. Cloots, Europhys. Lett. **24**, 629 (1993)
8. M. Kotrla, M. Predota, Europhys. Lett. **39**, 251 (1997); M. Kotrla, M. Predota, F. Slanina, Surf. Sci. **404**, 249 (1998); M. Kotrla, F. Slanina, M. Predota, Phys. Rev. B **58**, 10003 (1998)
9. M. Kardar, G. Parisi, Y.-C. Zhang, Phys. Rev. Lett. **56**, 889 (1986)
10. F. Léonard, M. Laradji, R.C. Desai, Phys. Rev. B **55**, 1887 (1997)
11. F. Léonard, R.C. Desai, Phys. Rev. B **55**, 9990 (1997)
12. B. Drossel, M. Kardar, Phys. Rev. Lett. **85**, 614 (2000)
13. R. Bausch, H.K. Janssen, H. Wagner, Z. Phys. B **24**, 113 (1976)
14. P.C. Hohenberg, B.I. Halperin, Rev. Mod. Phys. **49**, 435 (1977)
15. T. Halpin-Healy, Y.-C. Zhang, Phys. Rep. **254**, 215 (1995)
16. J. Krug, H. Spohn, Phys. Rev. Lett. **64**, 2332 (1990)
17. A.-L. Barabási, H.E. Stanley, *Fractal concepts in surface growth* (Cambridge University Press, 1995)
18. R.J. Glauber, J. Math. Phys. **4**, 294 (1963)
19. B. Drossel, M. Kardar, Phys. Rev. B **66**, 195414 (2002)
20. D.E. Wolf, L.-H. Tang, Phys. Rev. Lett. **65**, 1591 (1990)
21. B. Derrida, J.L. Lebowitz, E.R. Speer, J. Stat. Phys. **89**, 135 (1997)
22. D. Ertas, M. Kardar, Phys. Rev. Lett. **69**, 929 (1992)
23. M. Kardar, Physica A **263**, 345 (1999)
24. R. da Silveira, M. Kardar, Phys. Rev. E **68**, 046108 (2003), `cond-mat/0302003`
25. P.W. Rooney, A.L. Shapiro, M.Q. Tran, F. Hellman, Phys. Rev. Lett. **75**, 1843 (1995)